Dynamic Routing and Spectrum Allocation in Elastic Optical Networks With Mixed Line Rates

Xiong Wang, Kaixuan Kuang, Sheng Wang, Shizhong Xu, Hong Liu, and Gordon Ning Liu

***Abstract*—Elastic optical networks (EONs) are considered a very promising solution for next-generation optical networks. Elastic spectral bandwidth allocation promotes spectrum utilization efficiency and thus increases the network capacity. One of the fundamental problems in EONs is the routing and spectrum allocation (RSA) problem. Since real EONs may provide only a few regular line rates, we comprehensively study in this paper the dynamic RSA problem in EONs with several mixed line rates. To solve the dynamic RSA problem efficiently, we decompose the problem into RSA subproblems. For the routing subproblem, we propose an efficient multiconstrained routing algorithm named sorted feasible paths searching (SFPS) to find the shortest feasible paths for dynamic traffic demands. The completeness, optimality, and complexity of SFPS are proved. For the spectrum allocation subproblem, we propose two spectrum allocation strategies named fixed segmentation and adaptive segmentation to assign spectrum for the noncommensurate traffic demands of EONs with mixed line rates. Simulation results prove that the proposed dynamic RSA algorithms are time efficient and perform better than existing dynamic RSA algorithms in terms of bandwidth blocking probability and spectrum fragmentation ratio in EONs with mixed line rates.**

***Index Terms*—Dynamic traffic demands; Elastic optical network; Routing and spectrum allocation; Spectrum continuity constraints; Spectrum fragmentation; Transmission distance constraints.**

I. Introduction

Because of the popularity of video streaming, cloud computing services, and mobile applications, the traffic volume of the Internet is continually increasing [1]. The continuous growth of traffic volume presents significant challenges for Internet transport networks. To meet the increasing capacity requirement, wavelength-division multiplexing (WDM) systems with up to 40 or 100 Gb/s per channel have been deployed in backbone networks, while 400 Gb/s interfaces are now available in the laboratory [2]. Moreover, mixed line rate (10/40/100 Gb/s) WDM systems have also been deployed to serve heterogeneous traffic types at different data rates [3]. Thus, WDM optical transport networks seem to offer a practical and cost-effective solution for high capacity transport networks.

However, traditional WDM optical networks strictly follow the International Telecommunication Union (ITU-T) fixed uniform spacing and grid (typically at 50 or 100 GHz) [4], which will lead to low spectrum utilization efficiency. For example, an entire wavelength will be assigned to a lower rate traffic demand even if it will not fill the wavelength channel, whereas a group of wavelengths including guard bands between the adjacent wavelengths in the group may be assigned to a higher rate traffic demand. It is obvious that the inflexible grid and coarse bandwidth granularity of traditional WDM optical networks resulted in significant optical spectrum waste and a limited potential to improve network capacity.

To cope with the issues of underutilized spectrum and low agility in WDM networks, the elastic optical network (EON) architectures were proposed in recent years [5]. An EON has a spectrum slot (e.g., 12.5 GHz) much finer than that of 50 or 100 GHz ITU grid WDM systems and can also combine the spectrum slots to create wider channels on an as-needed basis. So to improve the spectrum utilization, the nodes in an EON may have mixed line rates, each of which requires a different number of spectrum slots. In theory, EONs are flexible enough to provide almost any line rate. However, real EONs may have only a few line rates. This is because (1) the spectrum fragments and management complexity are increased significantly with the number of line rates supported, and (2) real EONs are eventually upgraded from lower line rates to higher line rates (a large number of line rates coexisting is uncommon). Therefore, in this paper, we assume that EONs support only a limited number of mixed line rates. It is demonstrated that EONs with mixed line rate interfaces can accommodate heterogeneous traffic demands in a much more cost-efficient and spectrum-efficient [6] manner than that of WDM networks.

To accommodate a traffic demand in an EON, the control plane of the network must find a path and allocate sufficient spectrum on all the fiber links along the path to create an appropriately sized end-to-end optical path for the

Manuscript received June 20, 2014; revised October 20, 2014; accepted October 31, 2014; published November 26, 2014 (Doc. ID 214392).

X. Wang (e-mail: wangxiong@uestc.eu.cn), K. Kuang, S. Wang, and S. Xu are with the Key Lab of Optical Fiber Sensing and Communications (Ministry of Education), School of Communication and Information Engineering (SCIE), University of Electronic Science and Technology of China, Chengdu, China.

H. Liu and G. N. Liu are with Huawei Technologies Co. Ltd., Shenzhen, China.

http://dx.doi.org/10.1364/JOCN.6.001115

1943-0620/14/121115-13$15.00/0

connection. This is called the routing and spectrum allocation (RSA) problem. The RSA problem in EONs is more challenging than the traditional routing and wavelength allocation (RWA) problem in WDM networks, and the traditional RWA solutions [7,8] are no longer applicable in EONs. Instead of wavelengths, a traffic demand may request multiple contiguous spectrum slots, which will occupy a contiguous portion of spectrum on each fiber link passed by the demand. Also, without all-optical spectrum convertors, the assigned spectrum must be the same on all the fiber links passed by the traffic demand, which is referred to as the spectrum continuity constraint. Therefore, efficient RSA algorithms are necessary in EONs to avoid fragmentation of spectral resources into small noncontiguous spectral bands on fiber links [9]. Furthermore, the signal transmission distance and bandwidth are closely related to the signal modulation level. Thus, if the modulation level is adaptive in the EONs, the RSA problem will be extended to a routing, modulation-level, and spectrum-allocation (RMSA) problem. However, as the adaptive modulation-level assignment technology will not be employed at the first stage due to the increased cost and complexity, we consider only the RSA problem in this paper. However, our proposed algorithms can be easily extended to solve the RMSA problem.

The RSA problem is one of the important problems for EONs. According to the traffic pattern, the RSA problem can be further classified as a static RSA problem or a dynamic RSA problem. The static RSA problem arises during the network planning stage, where the traffic demands are known *a priori*, and the optimal or near-optimal RSA solution is computed off line based on the given traffic demands. While the dynamic RSA problem is encountered during the real-time network operation phase, where traffic demands arrive at and depart from the network dynamically in a random manner, when a traffic demand arrives at a network, the control plane of the network must immediately find a RSA solution for the traffic demand. Compared with the static RSA problem, the dynamic RSA problem is more challenging, because the traffic demands that will arrive at the network in the future are never known *a priori*. In addition, with the random arrival and departure of traffic demands, the available spectrum will be fragmented, which will lead to spectrum underutilization and potential high blocking probability in EONs. Thus, dynamic RSA algorithms should consider how to accommodate as many potential future demands as possible and how to reduce the spectrum fragmentations without *a priori* knowledge of the future demands.

In this work, we investigate the dynamic RSA problem in EONs with mixed line rates. We propose two novel spectrum allocation strategies that can efficiently reduce the spectrum fragmentation and enhance the spectrum utilization in EONs. Moreover, to find a path that satisfies the spectrum constraints and transmission distance constraint for each traffic demand, we propose an efficient multiconstrained routing algorithm. Meanwhile, in order to accommodate more potential traffic demands in networks under the dynamic scenario, we also evaluate several routing strategies in our routing algorithms.

The rest of the paper is organized as follows. The next section examines previous work and the main contributions of our work. Section III introduces the network model and constraints. Section IV presents our proposed multiconstrained routing algorithm, the routing strategies used in the routing algorithm, and the proposed spectrum allocation strategies. Section V gives the numerical analysis of the proposed RSA algorithms, and Section VI concludes this paper.

II. Related Work and Our Contributions

As an important problem for EONs, the RSA/RMSA problem under both static and dynamic scenarios has recently attracted much attention. The static RSA/RMSA problem is investigated in [10–16]. The static RSA/RMSA problem under the spectrum continuity constraints has been proved to be NP-complete [10,11]. Wang *et al.* [10] and Christodoulopoulos *et al.* [11] formulated integer linear programming models for the static RSA problem and the RMSA problem, respectively. The heuristic algorithms for the static RSA/RMSA problem are also proposed in [10–16]. To reduce the complexity of the RSA/RMSA problem, the heuristic algorithms proposed in [10–15] decompose the static RSA/RMSA problem into RSA subproblems and solve them sequentially. Regarding routing, the shortest path is used in [10] and the precalculated k shortest paths (KSP) are used in [10–15]. After routing, the first-fit (FF) [10–14] and maximize common large segment (MCLS) [15] spectrum allocation strategies are used to assign a portion of contiguous spectrum to each demand on the links that comprise the path of the demand. To find better solutions for the static RSA/RMSA problem, Patel *et al.* [16] used the genetic evolution and simulated annealing algorithm to optimize RSA.

The dynamic RSA/RMSA problem is investigated in [17–20]. In [17,18], the authors proposed two KSP-based dynamic RSA algorithms, which examine k shortest candidate paths for each traffic demand and then choose the one with available spectrum. Since the candidate paths are predetermined, the KSP-based RSA algorithms perform badly for dynamic traffic demands with routing constraints. To address the constrained routing issue, Wan *et al.* [19,20] proposed two dynamic RSA algorithms called modified shortest path (MSP) and spectrum-constraint path vector searching (SPV), respectively. MSP and SPV find the route and the available contiguous spectrum simultaneously. MSP is simply modified from Dijkstra's shortest path algorithm by adding checking operations for the RSA constraints, and SPV searches the shortest path that satisfies the RSA constraints for each traffic demand. However, the performance of MSP is unsatisfactory, and the computational complexity of SPV is very high. In addition, the studies reported in [17–20] assume that the traffic demands may have arbitrary bandwidth requirement, and the proposed algorithms are not appropriate for EONs with mixed regular line rates (e.g., 40/100/400 Gb/s).

Pages *et al.* [21] and Zhu *et al.* [22] proposed several multipath-routing-based dynamic RSA schemes in EONs. These RSA schemes allow a demand to be split into multiple demands and transmitted on multiple paths. Thus, multipath-routing-based RSA/RMSA schemes [21,22] can dramatically reduce the blocking probability of traffic demands compared with single-path-routing-based RSA/RMSA schemes [17–20]. However, for multipath routing, the differential delay between routing paths will lead to increased cost of network devices and network maintenance.

In dynamic scenarios, the available spectrum on the fiber links may be highly fragmented with dynamic optical path setup and release operations. To mitigate spectrum fragmentation effects in EONs, Moura *et al.* [23], Yin *et al.* [24], and Liu *et al.* [25] propose dynamic fragmentation aware routing and spectrum assignment algorithms, assuming the traffic demands may have an arbitrary bandwidth requirement. However, under an arbitrary bandwidth requirement, it is hard to reduce spectrum fragmentation. Furthermore, the proposed algorithms do not consider some important routing constraints (e.g., hop and distance). Another way to mitigate spectrum fragmentation effects is to use spectrum defragmentation mechanisms [26,27]. The basic idea of these spectrum defragmentation mechanisms is to properly rearrange active connections in the network, so as to release as much contiguous spectrum as possible. However, spectrum defragmentation operations will cause traffic disruptions, which are not admissible for certain classes of traffic.

In addition, the data rate/bandwidth variable capability of EONs brings inherit flexibility of supporting time-varying traffic with a transmission rate that fluctuates over time. Christodoulopoulos *et al.* [28,29] proposed dynamic spectrum allocation policies for time-varying traffic in EONs. Since the elastic RSA under time-varying demands puts additional requirements on network equipment and network control, the RSA for time-varying traffic is out of the scope of this paper.

In summary, although dynamic RSA in EONs is not a new topic, the existing studies still have some shortcomings, especially for EONs with a few mixed regular line rates. Based on the shortcomings of existing work, we in this paper comprehensively investigate the dynamic RSA problem in EONs with a few mixed line rates. The major contributions of this work are the following. i) We propose an efficient multiconstrained routing algorithm that can find the optimal paths for traffic demands efficiently, and we prove the completeness, optimality, and complexity of the proposed routing algorithm. ii) We evaluate the influence of different routing strategies on the traffic blocking probability, and find that a load balance routing strategy performs the best under dynamic scenarios. iii) In order to mitigate the spectrum fragmentation and reduce the traffic blocking probability, we propose two spectrum allocation strategies. The simulation results demonstrate that the proposed spectrum allocation strategies can mitigate spectrum fragmentation.

III. Network Model and the Dynamic RSA Problem in Eons With Mixed Line Rates

The architecture of EONs has been introduced in previous studies [5]. In this section we first briefly present the model of EONs, and then based on the network model, we present the dynamic RSA problem in EONs.

A. Network Model

An EON can be represented by an undirected graph $G = (V, E)$, where V and E denote the set of nodes and fiber links, respectively. All fiber links have the same contiguous spectral window $W = (f_{\text{start}}, f_{\text{end}})$, and $f_{\text{end}} - f_{\text{start}} = C$. The distance of the fiber link (u, v) is $D_{uv} km$. The EON supports a set of regular line rates, R. For example, $R = \{40\ \text{Gb/s}, 100\ \text{Gb/s}, 400\ \text{Gb/s}\}$. Each line rate $r \in R$ requires a spectral width of b_r GHz. A traffic demand, which requests a data rate of d Gb/s between source node s and termination node t, is denoted as $TD(s, t, d)$. To accommodate the traffic demand $TD(s, t, d)$, nodes s and t will use a transponder with a line rate of TD_r Gb/s ($d \le r$), and a light path with a spectral width of TD_{b_r} GHz also needs to be established between the two transponders. We define $\Lambda = \{b_r | r \in R\}$.

B. Dynamic RSA Problem in EONs With Mixed Line Rates

In dynamic scenarios, traffic demands randomly arrive at the network with unpredictable durations. When a traffic demand $TD(s, t, d)$ reaches an EON, the control plane of the EON needs to find a feasible path and allocate sufficient spectrum resources for the path. It is assumed that the RSA algorithm is implemented in centralized path computation elements (PCEs) or software defined network (SDN) controllers and that information about the status of spectrum availability is stored in the databases of SDN controllers or PCEs. Due to the physical limitation of the EON, the following constraints must be fulfilled when solving the RSA problem:

(C1) Transmission distance constraint. The quality of the optical signal will degrade with increasing transmission distance. To successfully recover the information at the destination node, the length of the light path must be less than a threshold $D_{\max}$.

(C2) Spectrum continuity constraint. The spectrum continuity constraint specifies that the light path should use the same contiguous portions of the spectrum on each fiber link traversed by it.

(C3) Spectrum nonoverlapping constraint. The spectrum nonoverlapping constraint ensures that the same portion of the spectrum in a fiber link cannot be assigned to different light paths.

(C4) Spectrum contiguousness constraint: The spectrum contiguousness constraint guarantees that the

spectrum allocated to a light path will be a contiguous portion on each link of the path.

To increase profit, network service providers prefer to accommodate as many traffic demands as possible, namely, reducing the traffic blocking probability. However, in practical networks, the importance of traffic demands may be different (depending on the bandwidth requirement). Thus, in this paper, the objective of the dynamic RSA algorithm is to minimize the bandwidth blocking probability (BBP), which is defined as

$$\text{BBP} = \frac{\sum_{TD} TD_{b_r} \cdot A_{TD}}{\sum_{TD} TD_{b_r}}, \tag{1}$$

where TD_{b_r} denotes the bandwidth required by traffic demand TD, and A_{TD} is a binary symbol indicating whether traffic demand TD is successfully accommodated or not ($A_{TD} = 1$ indicates that traffic demand TD is blocked; otherwise, demand TD is accepted).

IV. Dynamic RSA Algorithm

Since future traffic demands are unknown in dynamic scenarios, obtaining the global optimal RSA solution that has the minimum BBP is impossible. Thus, instead of finding a global optimal RSA solution for all traffic demands, we try to find an optimal RSA solution for each traffic demand based on the network status when the traffic demand arrives. To solve the dynamic RSA problem efficiently, we decompose the dynamic RSA problem into RSA subproblems and solve the two subproblems sequentially. For the routing subproblem, we propose an efficient multiconstrained shortest path algorithm, which can compute the shortest path that has available spectrum resources and satisfies the transmission distance constraint. The routing strategies will affect the BBP immensely. To find the best routing strategy under the dynamic scenario, we consider several routing strategies in our proposed routing algorithm. Finally, for the spectrum allocation problem, we propose two spectrum allocation strategies that can mitigate spectrum fragmentation on fiber links.

In this section, for ease of exposition, we first introduce some notation and assumptions used in the algorithms. Then we describe the multiconstrained routing algorithm and the routing strategies used in the routing algorithm. Last, we present the proposed spectrum allocation strategies.

A. Notation and Assumptions

w_{uv} denotes the cost of link (u, v). When a traffic demand arrives, the link costs are updated according to the routing strategy and network status. Let $\text{cost}(P_{xy})$ and $\text{dist}(P_{xy})$ denote the cost and length of a path P_{xy} from node x to node y, respectively. All fiber links have the same contiguous spectral window $W = (f_{\text{start}}, f_{\text{end}})$. C denotes the bandwidth of the fiber links ($C = f_{\text{end}} - f_{\text{start}}$). A spectrum segment ss is denoted as $(fs_{\text{start}}, fs_{\text{end}})$, where $fs_{\text{start}} \geq f_{\text{start}}$ and $fs_{\text{end}} \leq f_{\text{end}}$. With the random arrival and departure of traffic demands, the available spectrum resource on a fiber may be a set of noncontiguous spectrum segments. For example, in Fig. 1, when demands TD1 and TD3 leave, the spectrum segments ss1 and ss3 are available [Fig. 1(b)]. The set of available spectrum segments on a fiber link (u, v) is denoted as Ω_{uv}. Note that two spectrum segments contained in Ω_{uv} will not overlap. To precisely describe the RSA algorithm, we define the following primitive spectrum operations.

Belong to ($\in$) and not belong to ($\notin$). We say that a spectrum segment $ss = (fs_{\text{start}}, fs_{\text{end}}) \in \Omega$ if there exists a spectrum segment $\bar{ss}$ in Ω, such that $fs_{\text{start}} \geq \bar{fs}_{\text{start}}$ and $fs_{\text{end}} \leq \bar{fs}_{\text{end}}$. Otherwise, we say that $ss \notin \Omega$.

Intersection ($\bigcap$). The intersection operation calculates the overlapping spectrum segments of a set of two spectrum segments. For example, the intersection of $\bar{\Omega} = \{(10\ \text{GHz}, 60\ \text{GHz}), (120\ \text{GHz}, 150\ \text{GHz}), (200\ \text{GHz}, 240\ \text{GHz})\}$ and $\hat{\Omega} = \{(40\ \text{GHz}, 70\ \text{GHz}), (160\ \text{GHz}, 180\ \text{GHz}), (220\ \text{GHz}, 260\ \text{GHz})\}$ is {(40 GHz, 60 GHz), (220 GHz, 240 GHz}. The intersection of $\bar{\Omega}$ and $\hat{\Omega}$ is denoted as $\bar{\Omega} \bigcap \hat{\Omega}$.

Union ($\bigcup$). The union operation of $\bar{\Omega}$ and $\hat{\Omega}$ first puts all the spectrum segments in $\bar{\Omega}$ and $\hat{\Omega}$ to one set, and then merges the overlapped segments in the set into one segment. For example, $\bar{\Omega} = \{(10\ \text{GHz}, 60\ \text{GHz}), (120\ \text{GHz}, 150\ \text{GHz}), (200\ \text{GHz}, 240\ \text{GHz})\} \bigcup \hat{\Omega} = \{(40\ \text{GHz}, 70\ \text{GHz}), (160\ \text{GHz}, 180\ \text{GHz}), (220\ \text{GHz}, 260\ \text{GHz})\}$ is {(10 GHz, 70 GHz), (120 GHz, 150 GHz), (160 GHz, 180 GHz), (200 GHz, 260 GHz)}. The union of $\bar{\Omega}$ and $\hat{\Omega}$ is denoted as $\bar{\Omega} \bigcup \hat{\Omega}$.

Relative complement (\). The relative complement of $\hat{\Omega}$ in $\bar{\Omega}$ removes the intersection of $\bar{\Omega}$ and $\hat{\Omega}$ from $\bar{\Omega}$. For example, the relative complement of $\bar{\Omega} = \{(10\ \text{GHz}, 60\ \text{GHz}), (120\ \text{GHz}, 150\ \text{GHz}), (200\ \text{GHz}, 240\ \text{GHz})\}$ and $\hat{\Omega} = \{(40\ \text{GHz}, 70\ \text{GHz}), (160\ \text{GHz}, 180\ \text{GHz}), (220\ \text{GHz}, 260\ \text{GHz})\}$ is {(10 GHz, 40 GHz), (120 GHz, 150 GHz), (200 GHz, 220 GHz)}. The relative complement of $\bar{\Omega}$ in $\hat{\Omega}$ is denoted as $\bar{\Omega} \backslash \hat{\Omega}$.

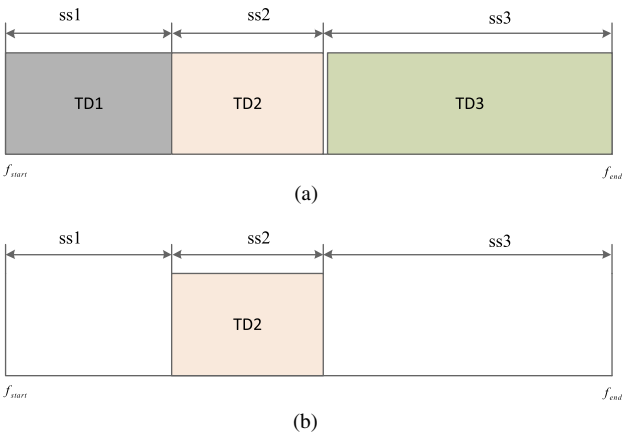

Fig. 1. Illustration for available spectrum segments.

Spectrum segments choose ($\Gamma(\Omega, b)$)**.** The spectrum segments choose operation removes spectrum segments whose bandwidth is less than b from Ω. For example, supposing $\Omega = \{(10\text{ GHz}, 70\text{ GHz}), (120\text{ GHz}, 140\text{ GHz}), (200\text{ GHz}, 240\text{ GHz})\}$, then $\Gamma(\Omega, 50) = \{(10\text{ GHz}, 70\text{ GHz})\}$.

The available spectrum segments set of a path P_{xy}, which is denoted as $\Omega_{P_{xy}}$, can be calculated by using spectrum intersection operations, i.e., $\Omega_{P_{xy}} = \bigcap_{(u,v)\in P_{xy}} \Omega_{uv}$.

B. Multiconstrained Routing Algorithm

In this subsection, we present the proposed multiconstrained routing algorithm used to find the shortest feasible path P_{st} for a traffic demand $TD(s,t,d)$. We say that a path P_{st} is feasible, if $\text{dist}(P_{st}) \le D_{\max}$ (i.e., P_{st} satisfies constraint C1) and $\Gamma(\Omega_{P_{st}}, TD_{b_r}) = \varnothing$ (i.e., P_{st} has available spectrum and satisfies constraints C2 to C4), where TD_{b_r} $(r \ge d)$ is the spectrum bandwidth requested by $TD(s,t,d)$.

The basic idea of our proposed multiconstrained routing algorithm is simple. It searches the feasible paths starting at node s and stores these paths in a container Q. In each iteration, a feasible path P_{su} is extracted from container Q, and if node u is not the termination node t, adjacent links of node u are explored to generate new feasible paths by augmenting P_{su} with these links and the newly generated feasible paths are inserted into container Q; otherwise, return to feasible path P_{st}. Initially, container Q stores only one path P_{ss}. To speed up the searching process and guarantee the optimality of the solution, the paths in Q are sorted in increasing order of their estimated cost. The estimated cost $f(P_{su})$ of a path P_{su} is defined as

$$f(P_{su}) = \text{cost}(P_{su}) + MC_{ut}, \tag{2}$$

where $\text{cost}(P_{su})$ is the actual cost of path P_{su}, and MC_{ut} is the cost of the shortest path from node u to node t without considering any constraint. Therefore, in each iteration, the first path in container Q will be extracted and used to expand feasible paths. We call the proposed algorithm the sorted feasible paths searching (SFPS) algorithm. The sorting operation, which is inspired by the A* shortest path algorithm [30], can significantly improve the efficiency of the path searching process. Since after sorting, the SFPS can return when it extracts a path that terminates at node t from container Q, the returned path is the feasible shortest path between nodes s and t, which will be proved blow. This means that SFPS does not need to explore all of the feasible paths between nodes s and t to find the optimal one.

Algorithm 1 Sorted Feasible Paths Searching

Input: The traffic demand $TD(s,t,d)$ and the bandwidth requirement TD_{b_r} of the demand.
Output: A shortest feasible path P_{st} from node s to node t.

```
1:  P_ss ← {s}, Ω ← {(f_start, f_end)}
2:  Q ← {P_st}
3:  while Q is not empty do
4:      remove the path P_su with the smallest estimated cost
        from Q
5:      if u==t then
6:          return P_su
7:      else
8:          for each adjacent link (u, v) of node u do
9:              if v ∉ P_su &&
                dist(P_su) + D_uv ≤ D_max &&
                Γ(Ω_{P_su} ⋂ Ω_uv, TD_{b_r}) ≠ φ then
10:                 insert path P_sv = P_su + (u, v) into Q
11:             end if
12:         end for
13:     end if
14: end while
15: return NULL
```

Algorithm 1 shows the detailed procedure in implementing the SFPS algorithm. The first step of SFPS is to update the link costs of the network. The link costs of the network are determined by the routing strategy. In this paper, we evaluate the following routing strategies.

Minimum hop routing (MHR). The MHR strategy selects the feasible path that has the smallest number of hops. When the link costs are set to the same value, shortest path routing reduces to minimum hop routing. For simplicity, we set the cost of all links to 1.

Load balance routing (LBR): The LBR routing strategy aims to distribute traffic demands uniformly among all the links. To achieve LBR, the cost of a link (u,v) is set to

$$w_{uv} = \frac{1}{C - UC_{uv}}, \tag{3}$$

where UC_{uv} is the used capacity of link (u,v).

Minimum interference routing (MIR): The MIR strategy [31] was first used in the dynamic traffic engineering algorithm for MPLS-based IP networks. The idea of MIR is that a newly routed traffic demand should follow a route that does not interfere with a route that may be critical for a future traffic demand, i.e., deferred loading of critical links. We assume that Ψ_{st} represents the set of the first k shortest paths for a node pair $\langle s,t\rangle$. A link (u,v) is defined as critical for a given node pair $\langle s,t\rangle$, if the link (u,v) is used by one path in Ψ_{st}. And $\delta_{st}(u,v)$ is an indicator of whether link (u,v) is critical for node pair $\langle s,t\rangle$. [If link (u,v) is critical for node pair $\langle s,t\rangle$, $\delta_{st}(u,v) = 1$, otherwise, $\delta_{st}(u,v) = 0$]. To achieve minimum interference routing, the cost of a link (u,v) is set to

$$w_{uv} = \sum_{s} \sum_{t=s} \delta_{st}(u,v). \tag{4}$$

Figure 2 illustrates how the SFPS calculates the shortest feasible path for a traffic demand $TD(A,E,100\text{ Gb/}s)$. We assume that the traffic demand requests a spectral bandwidth of 50 GHz, and the SFPS uses the MHR routing strategy. The cost, distance, and available spectrum segments of a link are labeled on the link. We assume that the maximum signal transmission distance of the traffic demand is 1500 km. Initially, path P_{AA} is added to set Q

[Fig. 2(b)]. In the first iteration, the path P_{AA} is extracted from Q and augmented by exploring the neighboring links of node A, and the feasible paths $P_{AB} = A \to B$ and $P_{AC} = A \to C$ are inserted into Q [Fig. 2(c)]. In the second iteration, path P_{AB}, which has the minimum estimated cost, is extracted from Q and augmented by exploring the neighboring links of node B, and the feasible paths $P_{AD} = A \to B \to D$ and $P_{AE} = A \to B \to E$ are inserted into Q [Fig. 2(d)]. Finally, the desired shortest feasible path $P_{AE} = A \to B \to E$ is obtained, and the algorithm terminates.

Theorem 1 (Completeness of SFPS): If there exist feasible paths from node s to node t, SFPS will find a feasible path from node s to node t.

Proof: We prove it by contradiction. We assume that there exist feasible paths from node s to node t, but SFPS cannot return a feasible path. With this assumption, the SFPS will terminate when set Q is empty. We assume that one of the feasible paths between nodes s and t is denoted as $s \to x_1 \cdots \to x_i \to x_{i+1} \cdots \to t$. It is clear that the feasible path $s \to x_1$ will be inserted into set Q when SFPS augments the path P_{ss}. Similarly, the feasible path $s \to \cdots \to x_i \to x_{i+1}$ will be inserted into set Q when SFPS augments the path $s \to \cdots \to x_i$. And thus, the feasible path $s \to x_1 \cdots \to x_i \to x_{i+1} \cdots \to t$ will be eventually added into Q. This contradicts the assumption.

Theorem 2 (Optimality of SFPS): If there exist feasible paths from node s to node t, SFPS will return the feasible path with the minimal cost.

Proof: If there exist feasible paths from node s to node t, the SFPS will stop and return path P^*_{st} when the termination of the path extracted from Q is node t. Since the termination of P^*_{st} is node t, $f(P^*_{st}) = \text{cost}(P^*_{st}) + MC_{tt} = \text{cost}(P^*_{st})$. We assume that P_{sx} is a feasible path in Q. It is obvious that when SFPS stops, $f(P^*_{st}) = \text{cost}(P^*_{st}) \le f(P_{sx})$ (Q is sorted). We also can prove that $\text{cost}(P^*_{st}) \le \text{cost}(P_{st})$, where $P_{st} \notin Q$ and $P_{st} = P^*_{st}$. We know that a feasible path P_{st} is generated by augmenting a feasible path P_{sx} in Q. From the definition of the estimated cost of a path, we can easily obtain that $MC_{xt} \le \text{cost}(P^*_{xt})$, where P^*_{xt} is the shortest feasible path from node x to t. Therefore, we have $f(P_{sx}) = \text{cost}(P_{sx}) + MC_{xt} \le \text{cost}(P_{sx}) + \text{cost}(P^*_{xt}) \le \text{cost}(P_{st})$. Furthermore, as the paths in Q are sorted in increasing order of their estimated cost, we have $\text{cost}(P^*_{st}) = f(P^*_{st}) \le f(P_{st})$. Thus, we can conclude that for any feasible path P_{st}, $\text{cost}(P^*_{st}) \le \text{cost}(P_{st})$, i.e., SFPS returns the shortest feasible path between nodes s and t.

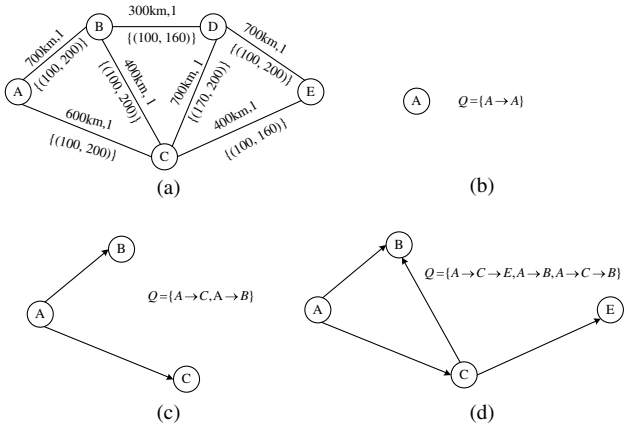

Fig. 2. Illustration of the SFPS algorithm.

Theorem 3 (Optimality of SFPS): The time complexity of SFPS is $O(K|E|\log(K|E|))$, where K is the maximum number of feasible paths between two nodes.

We assume that there are k_x different paths between nodes s and x. In each iteration, a path P_{sx} is extracted from Q, and ω_x adjacent links of node x will be checked, where ω_x is the degree of node x. Thus, in the worst case, at most $\sum_{x \in V} \omega_x \cdot k_x$ paths are inserted into set Q. Let $K = \max_{x \in V}\{k_x\}$. We have $\sum_{x \in V} \omega_x \cdot k_x = O(K \cdot \sum_{x \in V} \omega_x) = O(K \cdot |E|)$. We suppose that the set Q is implemented using a balanced binary tree, where operations such as path insertion and removal can be done in $O(|Q| \log |Q|)$. So the complexity of SFPS is $O(K|E|\log(K|E|))$. In practical networks, the K may be very large. Fortunately, the sorting operation in SFPS can dramatically decrease the number of paths in Q as well as the number of path augmentation operations.

C. Spectrum Allocation Strategies

Most RSA algorithms proposed in previous works employ the first-fit (FF) spectrum allocation strategy, which allocates the feasible spectrum segment with the lowest starting frequency among the set of feasible spectrum segments to a traffic demand. The FF strategy is very simple and performs well in traditional WDM networks. However, with random arrival and departure of traffic demands, the FF strategy will inevitably lead to spectrum fragments and high traffic blocking probability in EONs. We use the simple example in Fig. 3 to illustrate the drawback of the FF strategy. Suppose the spectral window of all the links is (100 GHz, 600 GHz), and a traffic demand will request a bandwidth in set $\Lambda = \{37.5\ \text{GHz}, 50\ \text{GHz}, 75\ \text{GHz}\}$. Initially, there are no traffic demands carried in the network. We assume that the first and second traffic demands, which both start at node A and end at node D and request a bandwidth of 50 GHz, arrive at the network at time $t1$ and $t2$ ($t2 > t1$), respectively. By using the FF strategy, the spectrum segments (100 GHz, 150 GHz) and (150 GHz, 200 GHz) on the links along the path $A \to B \to C \to D$ are assigned to the first and second traffic demands, respectively [Fig. 3(b)]. The first traffic demand leaves the network at time $\hat{t}1$ ($\hat{t}1 > t2$), and the spectrum segment (100 GHz, 150 GHz) on the links is released [Fig. 3(c)]. At time $t3$ ($t3 > \hat{t}1$), the third traffic demand from node A to node D, requesting a bandwidth of 37.5 GHz, arrives. The FF strategy allocates the spectrum segment (100 GHz, 137.5 GHz) on the links along the path $A \to B \to C \to D$ to the third traffic demand. Evidently, the available spectrum segment (137.5 GHz, 150 GHz) is a spectrum fragment [Fig. 3(d)], as it cannot be used by any traffic demand. From the above example, we observe that the spectrum fragments occur because traffic demands with different bandwidth requirements share the same portion of the

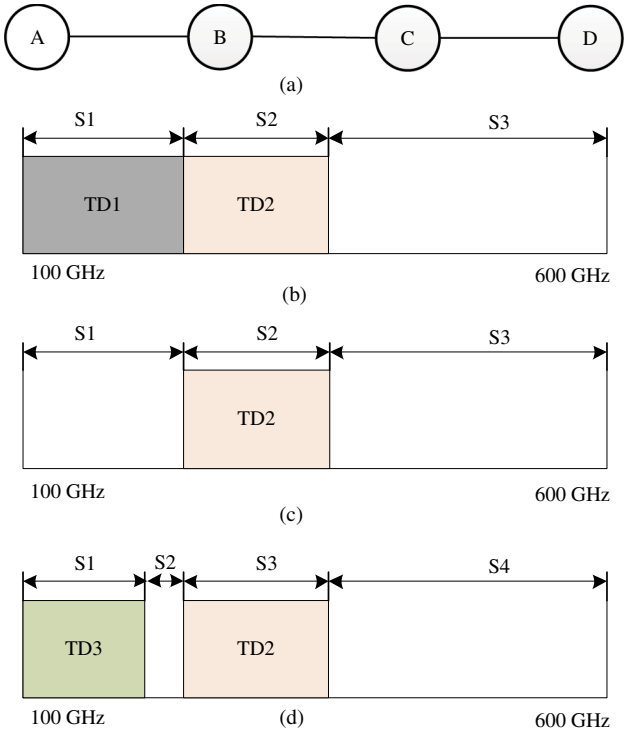

Fig. 3. Illustration of the FF strategy.

spectrum [e.g., the spectrum segment (100 GHz, 150 GHz) is used by two traffic demands with different bandwidth requirements]. Based on this observation, we can improve the FF strategy by introducing the spectrum segmentation strategy. The basic idea of the spectrum segmentation strategy is to partition the spectral window $W = (f_{\text{start}}, f_{\text{end}})$ of all links into several spectrum segments sets, and each spectrum segments set WS_{b_r} $(b_r \in \Lambda)$ is used to serve the traffic demands with a bandwidth requirement of b_r in priority. For the example in Fig. 3, the spectral window of all the links is partitioned into three segments sets: $WB_{37.5} = \{(100\text{ GHz}, 250\text{ GHz})\}$, $WB_{50} = \{(250\text{ GHz}, 450\text{ GHz})\}$, and $WB_{75} = \{(450\text{ GHz}, 600\text{ GHz})\}$, which are used to sever the traffic demands of 37.5, 50, and 75 GHz in priority, respectively. Specifically, when a traffic demand requesting a bandwidth of 37.5 GHz arrives, the spectrum allocation strategy first searches a feasible spectrum segment in $WB_{37.5}$, and only when a feasible spectrum segment is not found in $WB_{37.5}$, the spectrum allocation strategy will try to find a feasible spectrum segment in WB_{50} and WB_{75}. In this spectrum allocation strategy, the spectral window of a link is partitioned into spectrum segments sets in a fixed way. Thus, we call this spectrum allocation strategy the fixed segmentation (FS) spectrum allocation strategy. Algorithm 2 shows the detailed procedure of FS.

Algorithm 2 Fixed Segmentation

Input: The traffic demand $TD(s,t,d)$, the bandwidth requirement TD_{b_r}, the routing path P_{st} of $TD(s,t,d)$, the event type *Type* (equals *ARRIVAL* or *DEPARTURE*), and the spectrum segment *ss* occupied by $TD(s,t,d)$ (only for *DEPARTURE* event).

Output: For *ARRIVAL* event, output the spectrum segment *ss* allocated to $TD(s,t,d)$. For *DEPARTURE* event, output *NULL*.

1: **if** *Type*== *ARRIVAL* **then**
2: $ss \leftarrow \phi$
3: $\Omega_{p_{st}} \leftarrow \bigcap_{(u,v)\in P_{st}} \Omega_{uv}$
4: $\Omega_{temp} \leftarrow \Gamma(\Omega_{P_{st}} \bigcap WS_{TD_{b_r}}, TD_{b_r})$
5: **if** $\Omega_{temp} \neq \phi$ **then**
6: $ss \leftarrow (fs_{start}, fs_{start} + TD_{b_r}) \in \Omega_{temp}$
7: **else**
8: **for** each $b_r \in \Lambda$ and $b_r \neq TD_{b_r}$ **do**
9: $\Omega_{temp} \leftarrow \Gamma(\Omega_{P_{st}} \bigcap WS_{b_r}, TD_{b_r})$
10: **if** $\Omega_{temp} \neq \phi$ **then**
11: $ss \leftarrow (fs_{start}, fs_{start} + TD_{b_r}) \in \Omega_{temp}$ and **break**
12: **end if**
13: **end for**
14: **end if**
15: **for** each link $(u,v) \in P_{st}$ **do**
16: $\Omega_{uv} \leftarrow \Omega_{uv} \backslash ss$
17: **end for**
18: **return** ss
19: **end if**
20: **if** *Type*== *DEPARTURE* **then**
21: **for** each link $(u,v) \in P_{st}$ **do**
22: $\Omega_{uv} \leftarrow \Omega_{uv} \bigcup ss$
23: **end for**
24: **return** *NULL*
25: **end if**

In FS, the spectrum of all links is divided into several portions, each of which has a fixed spectrum bandwidth. However, the proportions of different traffic demand types are not known *a priori* in dynamic scenarios. Therefore, under dynamic scenarios, FS cannot sufficiently utilize the spectrum resource. To improve the performance of FS, we propose the adaptive segmentation (AS) spectrum allocation strategy. With the arrival of traffic demands, AS adaptively partitions the spectrum of all links into different portions. Let *BS* denote the blank spectrum set, which is defined as $BS = \bigcap_{(u,v)\in E} \Omega_{uv}$. Initially, $BS = \{(f_{\text{start}}, f_{\text{end}})\}$ and $WS_{b_r} = \phi$ $(b_r \in \Lambda)$. When a traffic demand with a bandwidth requirement of $TD_{b_r} \in \Lambda$ arrives, AS searches $WS_{TD_{b_r}}$, *BS*, and $WS_{b_r}(b_r \neq TD_{b_r})$ sequentially to find a feasible spectrum segment *ss* for the traffic demand. If a feasible spectrum segment *ss* is found and $ss \in BS$, let $WS_{TD_{b_r}} = WS_{TD_{b_r}} \bigcup ss$ and $BS = BS \backslash ss$. When a traffic demand with a bandwidth requirement of TD_{b_r} leaves, AS will first release the spectrum segment *ss* used by the traffic demand, and then update the *BS*. Algorithm 3 presents the detailed procedure of AS.

Algorithm 3 Adaptive Segmentation

Input: The traffic demand $TD(s,t,d)$, the bandwidth requirement TD_{b_r}, the routing path P_{st} of $TD(s,t,d)$, the event type *Type* (equals *ARRIVAL* or *DEPARTURE*), and the spectrum segment *ss* occupied by $TD(s,t,d)$ (only for *DEPARTURE* event).

Output: For *ARRIVAL* event, output the spectrum segment ss allocated to $TD(s,t,d)$. For *DEPARTURE* event, output *NULL*.

if $Type == ARRIVAL$ **then**
  $ss \leftarrow \phi$
  $\Omega_{p_{st}} \leftarrow \bigcap_{(u,v)\in P_{st}} \Omega_{uv}$
  $\Omega_{temp} \leftarrow \Gamma(\Omega_{P_{st}} \bigcap WS_{TD_{b_r}}, TD_{b_r})$
  if $\Omega_{temp} = \phi$ **then**
    $ss \leftarrow (fs_{start}, fs_{start} + TD_{b_r}) \in \Omega_{temp}$
  else
    $\Omega_{temp} \leftarrow \Gamma(\Omega_{P_{st}} \bigcap BS, TD_{b_r})$
    if $\Omega_{temp} \neq \phi$ **then**
      $ss \leftarrow (fs_{start}, fs_{start} + TD_{b_r}) \in \Omega_{temp}$
      $BS \leftarrow BS \backslash ss$
      $WS_{TD_{b_r}} \leftarrow WS_{TD_{b_r}} \bigcup ss$
    else
      for each $b_r \in \Lambda$ and $b_r \neq TD_{b_r}$ **do**
        $\Omega_{temp} \leftarrow \Gamma(\Omega_{P_{st}} \bigcap WS_{b_r}, TD_{b_r})$
        if $\Omega_{temp} \neq \phi$ **then**
          $ss \leftarrow (fs_{start}, fs_{start} + TD_{b_r}) \in \Omega_{temp}$ and **break**
        end if
      end for
    end if
  end if
  for each link $(u,v) \in P_{st}$ **do**
    $\Omega_{uv} \leftarrow \Omega_{uv} \backslash ss$
  end for
  return ss
  end if
  if $Type ==$ *DEPARTURE* **then**
    for each link $(u,v) \in P_{st}$ **do**
      $\Omega_{uv} \leftarrow \Omega_{uv} \bigcup ss$
    end for
    return *NULL*
  end if

V. Performance Evaluation

To evaluate the performance of the proposed algorithms, we have executed a series of simulations. In this section, we start by presenting the simulation setup, and then we evaluate the performance of the proposed algorithms through simulation results.

A. Simulation Setup

The discrete-event-based simulator and all the algorithms are implemented by using Microsoft Visual Studio 2008 and C++ programming language. All simulations are run on a computer with 4 GB memory and a 3 GHz CPU. Figure 4 shows the network topologies, TOPO-15 and USNET, we used in simulations for performance evaluation of the proposed algorithms. The traffic demands arrive dynamically, following a Poisson process with an average arrival rate λ per time unit, and the duration of each traffic demand follows the negative exponential distribution with an average of $\frac{1}{\mu}$ time unit. Therefore, the traffic load can be denoted as $\frac{\lambda}{\mu}$ in Erlangs. The source node and termination

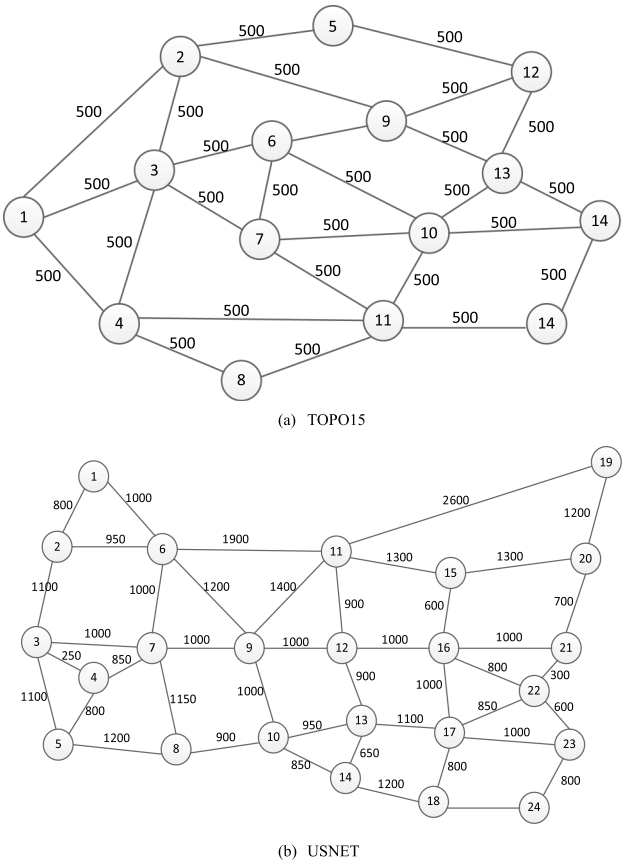

Fig. 4. Network topologies used for simulation

node of a traffic demand are uniformly distributed across the network. The bitrate of a traffic demand is randomly selected from set $\Lambda = \{40\ \text{Gb/s}, 100\ \text{Gb/s}, 400\ \text{Gb/s}\}$. The spectrum bandwidth requirements of 40, 100, and 400 Gb/s traffic demands are 37.5, 50, and 75 GHz, respectively. However, in some of the simulations, we also considered two spectral bandwidth options (75 and 100 GHz) for 400 Gb/s traffic demands. The transmission reaches of traffic demands are determined by the modulation methods. Based on the results reported in [2] and [32], the maximum transmission distances of 40, 100, and 400 Gb/s traffic demands are set to 3200 km (binary phase-shift keying modulation), 2500 km (quadrature phase-shift keying modulation), and 800 km (16-quadrature amplitude modulation), respectively. To extend the maximum reach of the traffic demands, we assume that 25% of the network nodes are deployed with regenerators. The regenerators are deployed in the nodes with higher degree. We assume that there is at least one path satisfying the transmission distance constraint between the source node and the destination node of a traffic demand (otherwise, the traffic demand will not be generated). The spectrum bandwidth of a fiber link is 5 THz. We compare our proposed dynamic RSA algorithms with three reference dynamic RSA algorithms, namely, SPV, MSR, and KSP [19,20]. The following metrics are used to evaluate the performance of the algorithms.

Bandwidth blocking probability (BBP). The definition of BBP is presented in Subsection III.B.

Spectrum fragmentation ratio (SFR). A spectrum fragment is a spectrum segment whose bandwidth is less than 37.5 GHz [33]. Thus, SFR is defined as

$$\mathrm{SFR} = \frac{\sum_{k=1}^{N}(\sum_{(u,v)\in E} SF_{uv}^{k})/C \cdot |E|}{N}, \tag{5}$$

where SF_{uv}^{k} is the total spectrum bandwidth of all spectrum fragments on link (u, v) when traffic demand k arrives.

Average computation time (ACT). ACT is defined as

$$\mathrm{ACT} = \frac{\sum_{k=1}^{N} CT_k}{N}, \tag{6}$$

where CT_k is the computation time of a RSA algorithm to find a route and allocate spectrum for traffic demand k.

B. Simulation Results

Figures 5(a) and 5(b) first show the simulation results on BBP of different routing strategies in the TOPO-15 and USNET topologies, respectively. We observe that the BBP curves in both figures follow the same trend. Among the three routing strategies, LBR achieves the lowest BBP and MHR has the highest BBP. The reason is that MHR seeks exclusively to minimize resource consumption, which may lead to unbalanced network resource usage and make the network partitioned, while the LBR will distribute traffic load uniformly among all the links, and thus can accommodate more potential demands. It is notable that intuitively, MIR seems the best routing strategy for dynamic scenarios; however, the simulation results indicate that MIR has higher BBP than LBR. The reason behind the results is that it is hard to precisely measure the critical links when a traffic demand arrives.

We then investigate the performance of FF, FS, and AS spectrum allocation strategies. We assume that in the routing stage, our proposed SFPS routing algorithm and the LBR routing strategy are employed. Figures 6(a) and 6(b)

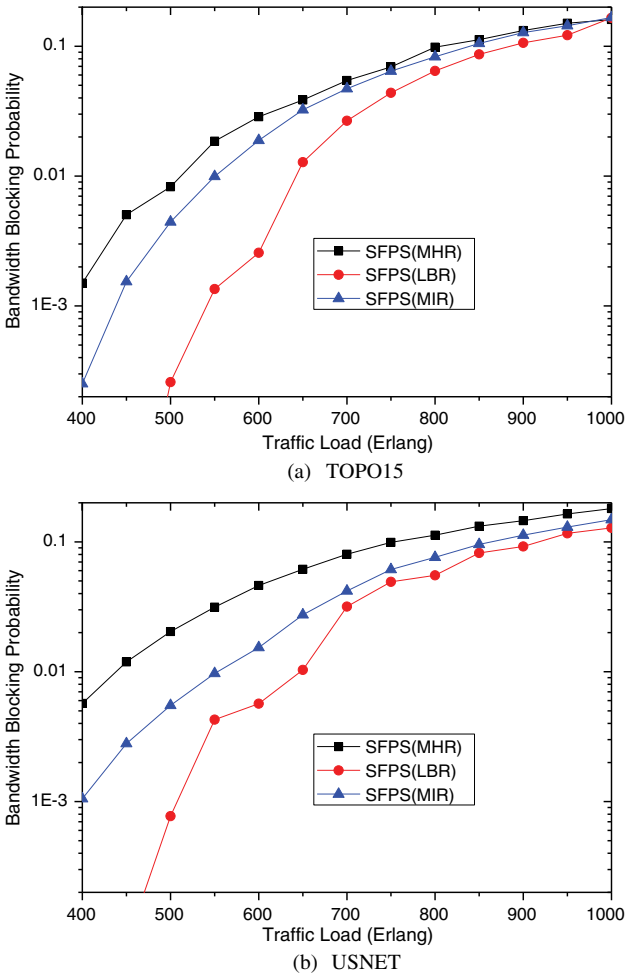

(a) TOPO15

(b) USNET

Fig. 5. BBP of different routing strategies in the (a) TOPO-15 and (b) USNET topologies.

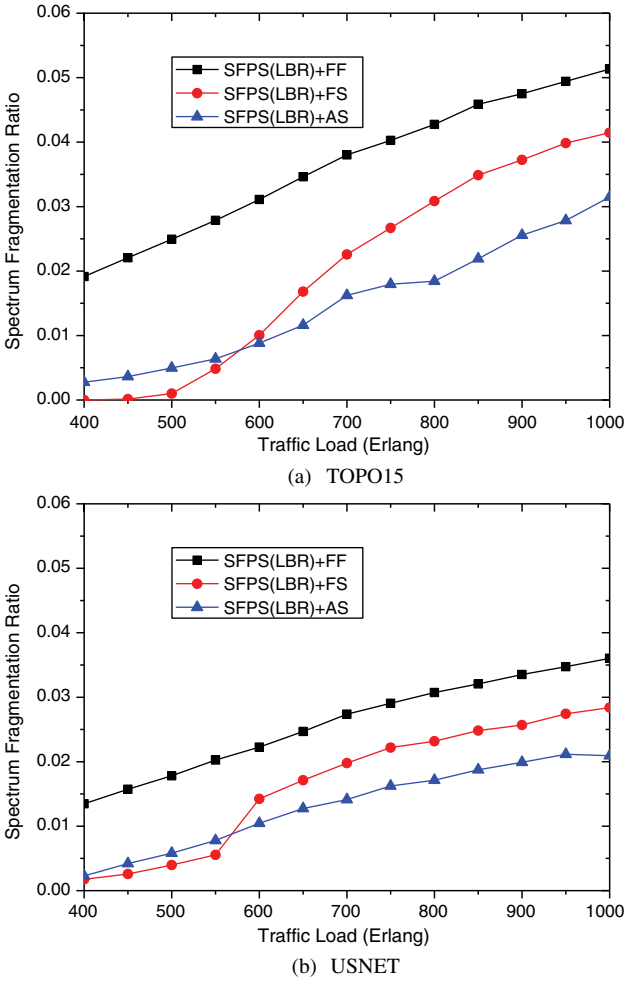

(a) TOPO15

(b) USNET

Fig. 6. SFR of different spectrum allocation strategies in the (a) TOPO-15 and (b) USNET topologies.

show the simulation results on SFR of different spectrum allocation strategies in the TOPO-15 and USNET topologies, respectively. The simulation results also follow the same trend in both topologies. As expected, the SFR of our proposed FS and AS is evidently lower than that of FF. We observe that when the traffic load is light, the SFR of FS is lower than that of AS, whereas when the traffic load becomes heavy, the SFR of FS is higher than that of AS. This is because when the traffic load is light, FS uses only the spectrum segments assigned to a traffic type to accommodate the traffic demands belonging to the traffic type (spectrum resource is enough), but as the traffic load becomes heavy, FS may use the spectrum segments assigned to a traffic type to accommodate the traffic demands not belonging the traffic type, which will lead to a highly fragmented spectrum.

We also compare the BBP of different spectrum allocation strategies in Fig. 7. Because the FS and AS have lower SFR than FF, the BPP of FS and AS is also lower than that of FF. The results in Figs. 6 and 7 demonstrate that FS and AS can improve the spectrum utilization efficiency, and thus can efficiently reduce the BBP of a network. From Figs. 6 and 7, we also find that FS performs better than AS under light traffic load, while AS performs better than FS under heavy traffic load.

Finally, we compare our proposed dynamic RSA algorithms with existing dynamic RSA algorithms, namely KSP, MSP, and SPV [19,20]. Figure 8 plots the simulation results on BBP of these algorithms in the two topologies. From Fig. 8, we can observe in both topologies, when the traffic load is medium or light (less than 850 Erlang), KSP has the highest BBP and our proposed RSA algorithms [SFPS(LBR)+FS and SFPS(LBR)+AS] achieve the lowest BBP. However, when the traffic load is heavy, all the algorithms obtain almost the same performance in terms of BBP. The reason is that KSP selects a feasible path for a traffic demand from a precalculated candidate path. Thus, under heavy traffic load, the path returned by KSP is always shorter than those returned by other algorithms. This means that KSP will block traffic demands with longer feasible paths and save spectrum resources for the traffic demands with shorter feasible paths. It is notable that in the TOPO-15 topology, the MSP and SPV obtain almost the same performance under all of the traffic loads, but in the USNET topology, the BBP of MSP is obliviously higher than that of SPV. The

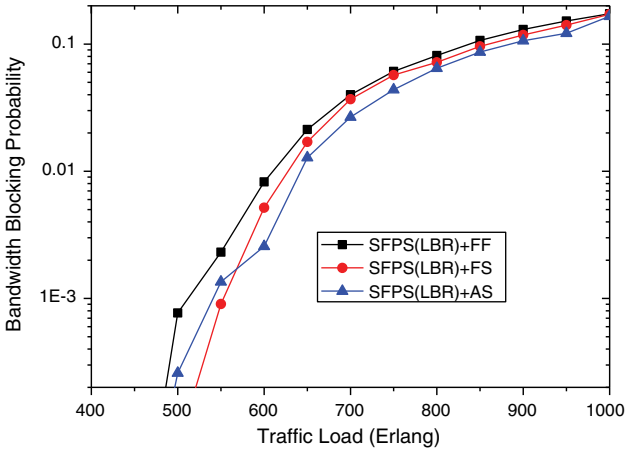

(a) TOPO15

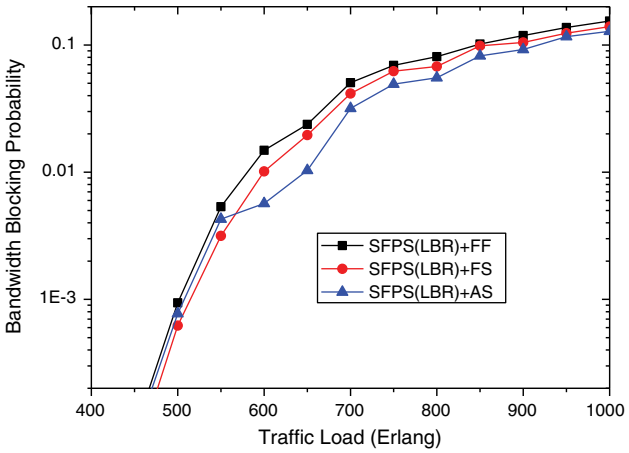

(b) USNET

Fig. 7. BBP of different spectrum allocation strategies in the (a) TOPO-15 and (b) USNET topologies.

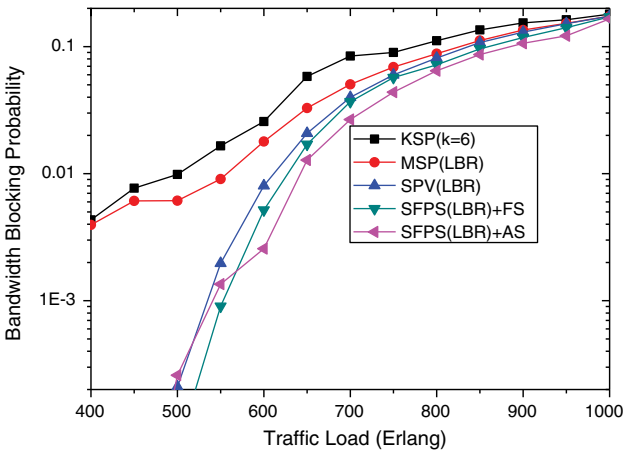

(a) TOPO15

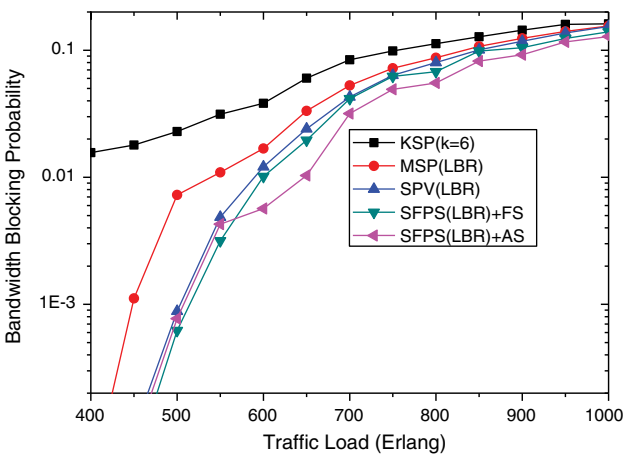

(b) USNET

Fig. 8. BBP of different dynamic RSA algorithms in the (a) TOPO-15 and (b) USNET topologies.

explanation is that the MSP is simply modified from Dijkstra's algorithm, and the feasible path searching capability of MSP is limited. The probability that MSP cannot find a feasible path increases dramatically with the increase of network size. Similar to the results in Fig. 7, under light or medium traffic load, SFPS(LBR)+FS performs better than SFPS(LBR)+AS, while under heavy traffic load, SFPS(LBR)+AS outperforms SFPS(LBR)+FS.

We also investigate the ACT of different RSA algorithms. The simulation results are presented in Fig. 9. SPV has the longest ACT, and the ACT of SPV increases significantly as the network size increases. In both of the topologies, the ACT required by our proposed SFPS(LBR)+FS and SFPS(LBR)+AS is slightly longer than the ACT required by the MSP. The KSP requires the shortest ACT, because the candidate paths are precalculated in KSP. We also can observe that the ACT required by SPV, MSP, SFPS (LBR)+FS, and SFPS(LBR)+AS decreases slowly with the increase of traffic load. The reason is that with the increase of traffic load, the size of the feasible solution space decreases; thus, the algorithm can find a feasible solution within a shorter time.

In intuition, the performance of our proposed algorithms will degrade with an increasing number of the bandwidth options. So, to evaluate the effects of bandwidth options on our proposed algorithms, we consider a scenario where 400 Gb/s traffic demands have two bandwidth options: 75 and 100 GHz. We assume that the maximum transmission distance of 400 Gb/s traffic demands modulated on 100 GHz bandwidth is 1000 km. Figure 10 shows the BBP of the algorithms. Comparing Fig. 10 with Fig. 8, we can see that the BBP of the algorithms increases with the number of bandwidth options. The reason is that the average required bandwidth and the spectrum fragmentation increases with the number of bandwidth options. As we discussed in Subsection IV.C, the FS spectrum allocation strategy cannot sufficiently utilize the spectrum resource since the spectrum segment assigned to each type of traffic demand is predetermined and fixed. Thus, from Fig. 10, we can also see that the BBP of SFPS(LBR)+FS increased significantly with the number of bandwidth options. For example, SFPS(LBR)+FS has almost the same BBP as SPV(LBR) when the traffic load is higher than 550 Erlang. However, we can also observe that SFPS

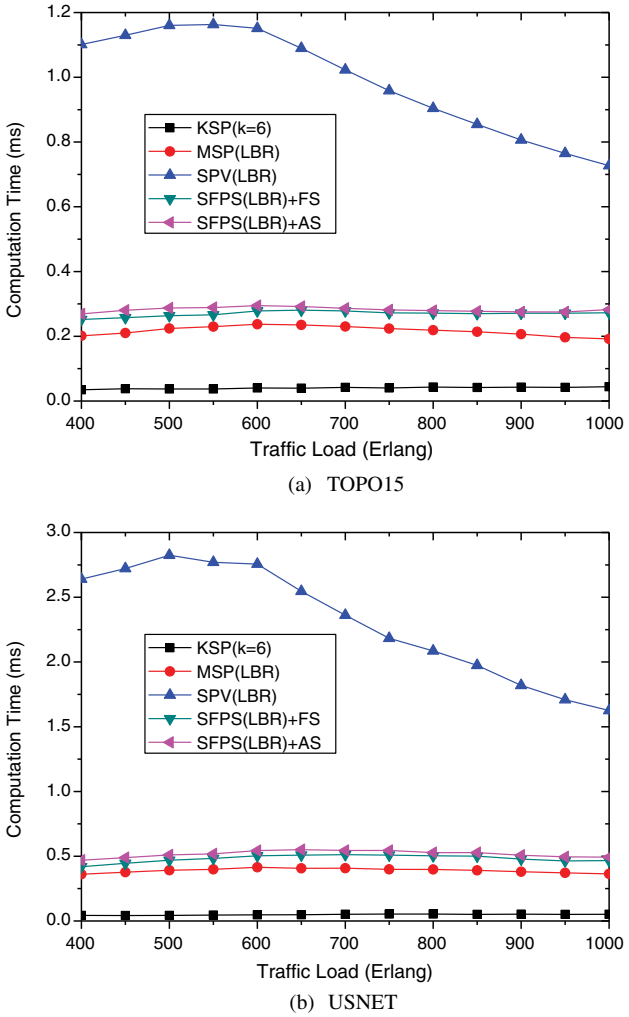

Fig. 9. ACT of different dynamic RSA algorithms in the (a) TOPO-15 and (b) USNET topologies.

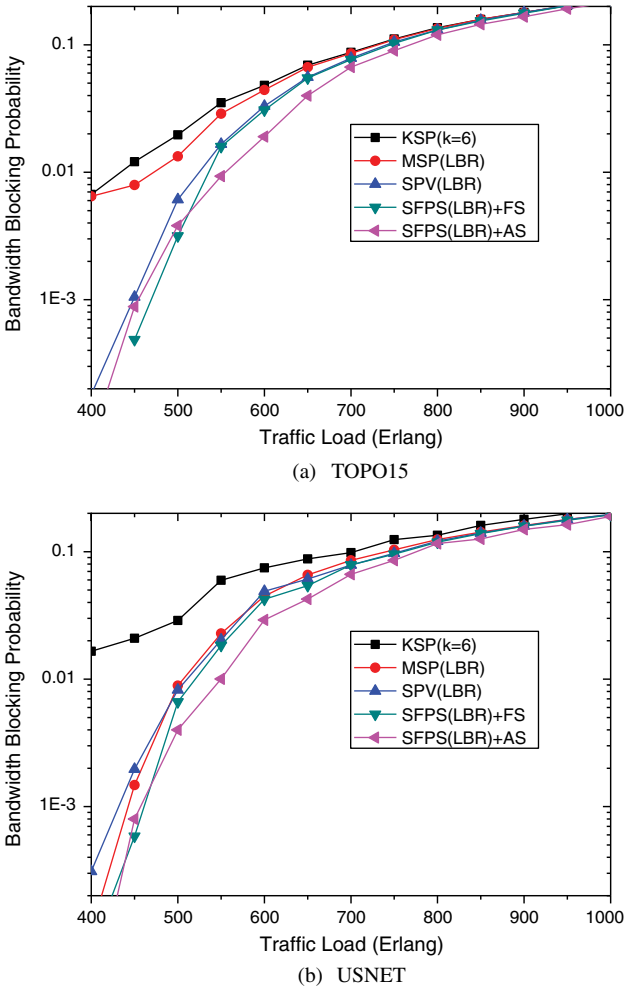

Fig. 10. BBP of different dynamic RSA algorithms in the (a) TOPO-15 and (b) USNET topologies when the bandwidth requirement set is (37.5 GHz, 50 GHz, 75 GHz, 100 GHz).

(LBR)+AS performs much better than other algorithms. This experiment demonstrates that the number of bandwidth options has significant impact on the performance of SFPS(LBR)+FS, while it has little impact on the performance of SFPS(LBR)+AS.

VI. Conclusion

In this paper, we investigated the dynamic RSA problem in EONs with mixed line rates. To efficiently solve the dynamic RSA problem, we used a two-stage approach. In the first stage, we proposed an efficient multiconstrained routing algorithm named SFPS to search feasible paths for traffic demands, and we also evaluated several routing strategies. The completeness and optimality of SFPS were proved. In the second stage, we proposed two spectrum allocation strategies, named FS and AS, to allocate spectrum to the feasible paths found in the first stage. FS and AS could reduce the spectrum fragmentation and traffic blocking probability. The proposed RSA algorithms were evaluated with numerical simulations using a Poisson traffic model and two mesh network topologies. The simulation results demonstrated that the proposed algorithms, SFPS(LBR)+FS and SFPS(LBR)+AS, could effectively reduce the spectrum fragmentation ratio and BBP of dynamic RSA, as compared to the existing algorithms. The simulation results also verified that the proposed algorithm is time efficient.

Acknowledgments

This work was partially supported by the 973 Program (2013CB329103), the NSFC Fund (61301153, 61271165, 61201128, 61201129), the Program for Changjiang Scholars and Innovative Research Team (PCSIRT) in University, 111 Project B14039, and the O of UESTC.

References

[1] A. A. M. Saleh and J. M. Simmons, "Technology and architecture to enable the explosive growth of the Internet," *IEEE Commun. Mag.*, vol. 49, no. 1, pp. 126–132, Jan. 2011.

[2] L. Zong, G. N. Liu, A. Lord, Y. R. Zhou, and T. Ma, "40/100/400 Gb/s mixed line rate transmission performance in flexgrid optical networks," in *Optical Fiber Communication Conf.*, Anaheim, CA, 2013.

[3] T. Wuth, M. W. Chbat, and V. F. Kamalov, "Multi-rate (100G/40G/10G) transport over deployed optical networks," in *Optical Fiber Communication Conf.*, San Diego, CA, 2008.

[4] "Spectral grids for WDM applications: DWDM frequency grid," ITU-T Recommentation G.694.1, 2006.

[5] M. Jinno, H. Takara, B. Kozicki, Y. Tsukishima, Y. Sone, and S. Matsuoka, "Spectrum efficient and scalable elastic optical path network: Architecture, benefits, and enabling technologies," *IEEE Commun. Mag.*, vol. 47, no. 11, pp. 66–73, 2009.

[6] A. Morea and O. Rival, "Efficiency gain from elastic optical networks," in *Optical Fiber Communication Conf.*, Los Angeles, CA, 2011.

[7] H. Zang, J. P. Jue, and B. Mukherjee, "A review of routing and wavelength assignment approaches for wavelength-routed optical WDM networks," *Opt. Netw. Mag.*, vol. 1, no. 1, pp. 47–59, 2000.

[8] R. Ramaswami and K. N. Sivarajan, "Routing and wavelength assignment in all-optical networks," *IEEE Trans. Netw.*, vol. 3, no. 5, pp. 489–500, 1995.

[9] Y. Zhao, J. Zhang, X. Shu, J. Wang, and W. Gu, "Routing and spectrum assignment in OFDM-based bandwidth-variable optical networks," in *Opto-Electronics and Communications Conf.*, 2011, pp. 543–544.

[10] Y. Wang, X. Cao, and Y. Pan, "A study of the routing and spectrum allocation in spectrum-sliced elastic optical path networks," in *IEEE Int. Conf. on Computer Communications*, 2011.

[11] K. Christodoulopoulos, I. Tomkos, and E. A. Varvarigos, "Routing and spectrum allocation in OFDM-based optical networks with elastic bandwidth allocation," in *IEEE Global Telecommunications Conf.*, 2010.

[12] M. Jinno, B. Kozicki, H. Takara, A. Watanabe, Y. Sone, T. Tanaka, and A. Hirano, "Distance-adaptive spectrum resource allocation in spectrum-sliced elastic optical path network," *IEEE Commun. Mag.*, vol. 48, no. 8, pp. 138–145, 2010.

[13] M. Klinkowski and K. Walkowiak, "Routing and spectrum assignment in spectrum sliced elastic optical path network," *IEEE Commun. Lett.*, vol. 15, no. 8, pp. 884–886, 2011.

[14] K. Christodoulopoulos, I. Tomkos, and E. A. Varvarigos, "Elastic bandwidth allocation in flexible OFDM-based optical networks," *J. Lightwave Technol.*, vol. 29, no. 9, pp. 1354–1366, 2011.

[15] Y. Sone, A. Hirano, A. Kadohata, M. Jinno, and O. Ishida, "Routing and spectrum assignment algorithm maximizes spectrum utilization in optical networks," in *European Conf. and Exhibition on Optical Communication*, 2011.

[16] A. N. Patel, P. N. Ji, and T. Wang, "A naturally-inspired algorithm for routing, wavelength assignment, and spectrum allocation in flexible grid WDM networks," in *IEEE GLOBECOM Workshop on Flexible Optical Networks*, 2012.

[17] H. Ding, M. Zhang, J. Xie, Y. Wang, F. Ye, L. Zhang, and X. Chen, "Dynamic routing and frequency slot allocation in elastic optical path network using adaptive modulations with consideration of both spectrum availability and distance," in *Asia Communications and Photonics Conf. and Exhibition*, 2011.

[18] R. Casellas, R. Munozu, J. M. Fabrega, M. S. Moreolo, R. Martinez, L. Liu, T. Tsuritani, and I. Morita, "Design and experimental validation of a GMPLS/PCE control plane for elastic CO-OFDM optical networks," *IEEE J. Sel. Areas Commun.*, vol. 31, no. 1, pp. 49–61, 2013.

[19] X. Wan, N. Hua, and X. Zheng, "Dynamic routing and spectrum assignment in spectrum-flexible transparent optical networks," *J. Opt. Commun. Netw.*, vol. 4, no. 8, pp. 603–613, 2012.

[20] X. Wan, L. Wang, N. Hua, H. Zhang, and X. Zheng, "Dynamic routing and spectrum assignment in flexible optical path networks," in *Optical Fiber Communication Conf.*, 2011.

[21] A. Pages, J. Perello, and S. Spadaro, "Lightpath fragmentation for efficient spectrum utilization in dynamic elastic optical networks," in *Int. Conf. on Optical Networking Design and Modeling*, Colchester, UK, 2012.

[22] Z. Zhu, W. Lu, L. Zhang, and N. Ansari, "Dynamic service provisioning in elastic optical networks with hybrid single-/multi-path routing," *J. Lightwave Technol.*, vol. 31, no. 1, pp. 15–22, 2013.

[23] P. M. Moura, N. L. S. Fonseca, and R. A. Scaraficci, "Fragmentation aware routing and spectrum assignment algorithm," in *IEEE Int. Conf. on Computer Communications*, 2014.

[24] Y. Yin, M. Zhang, Z. Zhu, and S. J. B. Yoo, "Fragmentation-aware routing, modulation and spectrum assignment algorithms in elastic optical networks," in *Optical Fiber Communication Conf.*, 2013.

[25] L. Liu, Y. Yin, M. Xia, M. Shirazipour, Z. Zhu, R. Proietti, Q. Xu, S. Dahlfort, and S. J. B. Yoo, "Software-defined fragmentation-aware elastic optical networks enabled by OpenFlow," in *European Conf. and Exhibition on Optical Communication*, 2013.

[26] Y. Yin, K. Wen, D. J. Geisler, R. Liu, and S. J. B. Yoo, "Dynamic on-demand defragmentation in flexible bandwidth elastic optical networks," *Opt. Express*, vol. 20, no. 2, pp. 1798–17804, 2012.

[27] T. Takagi, H. Hasegawa, K. Sato, Y. Sone, A. Hirano, and M. Jinno, "Disruption minimized spectrum defragmentation in elastic optical path networks that adopt distance adaptive modulation," in *Opto-Electronics and Communications Conf.*, 2011.

[28] K. Christodoulopoulos, I. Tomkos, and E. Varvarigos, "Dynamic bandwidth allocation in flexible OFDM-based networks," in *Optical Fiber Communication Conf.*, 2011.

[29] K. Christodoulopoulos, I. Tomkos, and E. Varvarrigos, "Time-varying spectrum allocation policies and blocking analysis in flexible optical network," *IEEE J. Sel. Areas Commun.*, vol. 31, no. 1, pp. 13–25, 2013.

[30] P. E. Hart, N. J. Nilsson, and B. Raphael, "A formal basis for the heuristic determination of minimum cost paths," *IEEE Trans. Syst. Sci. Cybernet.*, vol. 4, no. 2, pp. 100–107, 1968.

[31] M. Kodialam and T. V. Lakshman, "Minimum interference routing with applications to MPLS traffic engineering," in *IEEE Int. Conf. on Computer Communications*, 2000, vol. 2, pp. 884–893.

[32] M. H. Eiselt, H. Griesser, A. Autenrieth, B. T. Teipen, and J. Elbers, "Programmable modulation for high-capacity networks," in *Opto-Electronics and Communications Conf.*, 2012.

[33] E. Tsardinakis, A. Loard, P. Wright, G. Liu, and P. Bayvel, "Should like demands be grouped in mixed line rate networks?" in *Optical Fiber Communication Conf.*, 2013.